Phosphorus immobilization in Al–drinking water treatment sludge (Al–DWTS) and soil under laboratory conditions

W.C. LI AND Y.Q. ZHAO*

Centre for Water Resources Research, School of Architecture, Landscape and Civil Engineering,
University College Dublin, Newstead, Belfield, Dublin 4, Ireland

*** Corresponding Author:**

Name: Y.Q. Zhao
E-mail: yaqian.zhao@ucd.ie
Phone: +353-1-7163215
Fax: +353-1-7163297
Address: Centre for Water Resources Research, School of Architecture, Landscape and Civil
Engineering, University College Dublin, Belfield, Dublin 4, Ireland

Abstract: This study assessed the potential reuse of an aluminium coagulated drinking–water treatment sludge (Al–DWTS) as a main substrate in constructed wetland to replace soil for the treatment of P-enriched wastewater. The adsorption isotherm and kinetics of phosphorus (P) removal from high-P solution by Al–DWTS and a local soil from Bailieborough, Ireland, were studied and compared under laboratory conditions. Data of P adsorption were well fitted to the Langmuir and the Freundlich isotherms but the Freundlich isotherm had a higher correlation coefficient. The maximum P adsorption capacity of the Al–DWTS and the soil was 39.4 mg P mg^{-1} and 9.5 mg P mg^{-1}, respectively, at conditions of pH of 4.0 and temperature of 23 ℃. Kinetics studies show that adsorption in both cases followed pseudo-second-order kinetics. The fact that the Al–DWTS exhibited a significantly higher P adsorption capacity at high–P solution compared with the soil suggests that Al–DWTS can be a “novel–waste” bioadsorbent with promising application in wastewater treatment engineering, such as constructed wetland systems.

Keywords: adsorption, alum–drinking water treatment sludge; phosphorus; soil; wastewater treatment

1. Introduction

In recent years, much attention has been paid to phosphorus (P) pollution, its causes, ecological effects and the costs of clean up. Phosphorus enters the natural waters from various industries, domestic sewage, laundries, running water over phosphate rocks and extensive application of manure and fertilizers in agriculture. Typically, domestic wastewater has a total P concentration of approximately 10 mg P L^{-1}. The principal forms of phosphate are orthophosphate (5 mg P L^{-1}), pyrophosphate (1 mg P L^{-1}), and tripolyphosphate (3 mg P L^{-1}), together with smaller amounts of organic phosphate [1]. It is now necessary to adopt effective methods for the removal of P from wastewater before discharge, in order to meet the effluent limits of 0.5–1.0 mg P L^{-1} [2]. Reducing P levels in wastewater may be achieved by various techniques, such as enhanced biological P removal; traditional chemical precipitation with aluminium, calcium and iron salts and various physicochemical methods including reverse osmosis, electrodialysis, contact filtration and adsorption, etc. [3]. In recent decades, many researchers have investigated removal of phosphate from wastewater using adsorption techniques with various adsorbents and bioadsorbents such as activated aluminium oxide, half–burnt dolomite, soil, tamarind nut shell activated carbon [4], fly ash [5, 6], iron oxide tailings [7], blast furnace slag [8], recycled Fe(III)/Cr(III) hydroxide [9].

Drinking–water treatment sludge (DWTS), is a resultant byproduct generated in the process of using aluminium– or iron–based salts as coagulants during the production of drinking water. DWTS mainly consists of suspended solids (in terms of turbidity), silt particles, organic matter (in terms of colour) and microorganisms from source water, together with residual chemicals (coagulants, polyelectrolytes and conditioning agents) that are added during the treatment processes. DWTS is classified as high plasticity organic clay. In most cases worldwide, DWTS is disposed of as waste to landfill. Nevertheless, the application of DWTS in P immobilization has been increasingly studied to convert it from a “waste” into low cost bioadsorbents for beneficial reuse. It is now clear that DWTS can be used as a soil amendment to increase considerably the P sorption capacity of soil for reducing offsite P transport [10–12]. Research has demonstrated that a P–binding capacity of approximately 12.5 g P kg^{-1} DWTS can be achieved [13]. A higher capacity up to 37.0 g P kg^{-1} DWTS was reported by Dayton and Basta [14] in examining 18 DWTSs in the US.

Recent study by our group in University College Dublin, Ireland focused on exploiting and developing novel reuses of DWTS as raw material in civil and environmental engineering. Results have shown some remarkable potential in DWTS for immobilizing a wide range of P species from simulated P–enriched wastewater. Considerable amounts of P can be adsorbed onto a relatively low mass of DWTS [15, 16]. Furthermore, the DWTS has been tested as the first of its kind as main substrate in a constructed wetland system for treating animal farm wastewater with high P levels [17, 18]. Since the main substrate in constructed wetland is normally soil, sand or gravel [19], the use of easily and locally available DWTS not only provides a low cost technological solution of improving P removal, but also an effective DWTS management option for its beneficial reuse.

The objective of our research was to evaluate the P sorption capacity of an aluminium–coagulated DWTS (termed as Al–DWTS) under the condition of using a high–P solution. Emphasis was placed on the comparative study of P–adsorption behaviour and capacity between the Al–DWTS and a local soil obtained from Bailieborough, Ireland. The soil has previously been employed as the main substrate in a full-scale constructed wetland system for an agricultural–industry wastewater treatment. We investigated the equilibrium and kinetics of adsorption of P onto the Al–DWTS and the soil. We used the Langmuir and Freundlich models to fit the equilibrium isotherms at different temperatures. We analysed the kinetics of adsorption using pseudo-first-order, pseudo-second-order and intra-particle diffusion models.

2. Materials and methods

2.1. Al–DWTS, soil and P solution preparation

The Al–DWTS was the brownish-green residual produced at the Ballymore–Eustace Water Treatment Plant located in South Dublin, Co. Kildare, Ireland from the treatment of a medium colour, medium turbidity, raw water that had been sourced from the Dublin and Wicklow mountains (upland catchments of peat over granite bedrock), and stored in Poulaphouca reservoir, County Wicklow. Dewatered Al–DWTS samples were collected from the dewatering unit of the plant, which uses aluminium sulphate as main coagulant with a dose of 42–60 mg L^{-1} for flocculation. The soil samples were obtained from the top 10 cm soil of the agricultural land at Lakeland Dairies, Bailieborough, County Cavan, Ireland, where the same soil has been used for constructing a full-scale constructed wetland system treating a cheese industry effluent. The Al–DWTS and soil were air–dried, ground and sieved through a 150 μm sieve size. The major element components of the Al–DWTS and soil were determined mainly by ICP–analysis and listed in Table 1. This shows that the Al–DWTS contains an abundant amount of Al (24,880 mg kg^{-1} DM (dry mass)) with significant level of organics indicated by the loss of ignition, which ranged 49–57%. This may be attributed to humic substances contained in the treated source water. Relatively, the soil contains much less Al (5,409 mg kg^{-1} DM) and high P (2,400 mg kg^{-1} DM), S (4,759 mg kg^{-1} DM) and Mg (3,696 mg kg^{-1} DM). This may be due to the Irish peat land nature. The stock solution of P was prepared in distilled water using potassium dihydrogen phosphate (KH_2PO_4). All working solutions were prepared by diluting the stock solution with distilled water.

2.2. Procedures and analysis

P–sorption experiments were conducted by equilibrating 3 g each of Al–DWTS and soil with 30 mL of varying P concentration in 150 mL plastic bottles. The bottles were then placed on a Stuart Orbital Shaker (SSL 1, Bibby Sterilin Ltd) and the mixture was agitated at 200 rpm for 6 h to ensure equilibrium. The pH values of the suspensions were adjusted to 3.0, 4.0, 5.5, 7.0, and 9.0 using either HNO_3 or NaOH. After equilibration, samples were filtered using a 0.45 Millipore membrane filter to separate the solids from the liquid and the residual P concentration was measured according to method 8114 (HACH) using a HACH DR/2400 spectrophotometer [16]. For the isotherm studies, six levels of initial phosphate concentrations (69; 343; 856; 1,142; 1,712; 3,425 mg P L^{-1}) were used while the pH was maintained at an adjusted value of 4.0. Kinetic studies were also carried out at pH 4.0 using 3 g of the adsorbent and six different initial concentrations. The effect of temperature on adsorption equilibrium was investigated by conducting the shaking experiment in an oven with temperature varying from 23 to 37 °C.

3. Results

3.1. Effect of contact time and concentration

In order to establish equilibrium time for maximum adsorption and also investigate the kinetics of the adsorption process, the adsorption of P on the Al–DWTS and the soil at various initial concentrations was studied as a function of contact time. Figs 1 and 2 show the results. Figure 1 shows that the equilibrium time for the adsorption of phosphate by Al–DWTS was 2 h when the P concentration (C_0) ranged from 69 to 1,712 mg P L^{-1}, while for an initial concentration of 3,425 P mg L^{-1}, the equilibration time was 6 h. Figure 2 indicates that the equilibrium adsorption by soil can be attained in 2 h when the initial P concentrations are below 1,142 mg P L^{-1}. Accordingly, 4 h is required to reach the equilibrium adsorption when the initial P concentrations are 1,712 mg P L^{-1} and 3,425 mg P L^{-1}, as shown in Fig. 2. Both the figures exhibit a rapid adsorption trend at the instant of contact. For instance, 50% adsorption on Al–DWTS was completed within 0.5 h for 3,425 mg P L^{-1} and within less than 0.25 h for the soil. Table 2 shows the effect of different initial concentrations on P adsorption ability by Al–DWTS and soil. The amount of P absorbed per unit mass (q_t) of Al–DWTS and soil seems to increase with an increased C_0, whereas an exception was observed at P initial concentration of 3,425 mg L^{-1} for soil adsorption.

3.2. Effect of pH

Figure 3 presents the effect of pH on the P adsorption by Al–DWTS and soil. Figure 3 shows that the optimum pH for both Al–DWTS and soil is 4.0. This corresponds to adsorption capacities of 31.6 mg P g^{-1} and 8.2 mg P g^{-1} for Al–DWTS and soil, respectively. Adsorption at pH 9.0 was the least, with a corresponding adsorption capacity of 14.7 mg P g^{-1} and 2.9 mg P g^{-1} for Al–DWTS and soil, respectively. The results indicate that the P adsorption onto Al–DWTS and soil is a physicochemical process and the adsorption ability is strongly dependent upon solution pH. The adsorptions are favoured in the acidic range with adsorption maxima obtained at pH 4.0 for both Al–DWTS and soil.

3.3. Kinetics study

The kinetics of P adsorption onto Al–DWTS and soil were studied using two models: pseudo-first- and second-order kinetics.

3.3.1. Pseudo-first-order model

The pseudo-first-order equation is given as:

$$\frac{dq_t}{dt} = k_1(q_e - q_t) \tag{1}$$

where q_t is the amount of adsorbate adsorbed at time t (mg g^{-1}), q_e the adsorption capacity at equilibrium (mg g^{-1}), k_1 the pseudo-first-order rate constant (h^{-1}) and t the contact time (h). The integration of Eq. (1) with the initial condition, $q_t = 0$ at $t = 0$ leads to:

$$\log(q_e - q_t) = \log q_e - \frac{k_1}{2.303}t \tag{2}$$

The values of the adsorption rate constant (k_1) for P were determined from the plot of $\log(q_e - q_t)$ against t.

3.3.2. Pseudo-second-order model

The pseudo-second-order model is described as below [20]:

$$\frac{dq_t}{dt} = k_s(q_e - q_t)^2 \tag{3}$$

After integration by applying the boundary conditions, Eq. (3) becomes:

$$q_t = \frac{tk_s q_e^{\ 2}}{1 + tk_s q_e} \tag{4}$$

The initial sorption rate, r (mg/g h), at $t \to 0$ is defined as

$$r = k_s q_e^{\ 2} \tag{5}$$

Eq. (4) can then be rearranged to obtain

$$q_t = \frac{t}{1/r + (1/q_e)t} \tag{6}$$

Thus q_e can be obtained from the slope of t/q_t versus t and r is obtained from the intercept. Therefore, k_s can be calculated from Eq. (5). Figures 4 and 5 show the plot of Eq. (6) for adsorption of P onto Al–DWTS and soil, respectively. The results demonstrate a linear relationship between adsorbed phosphate and t, with high correlation coefficients. The kinetic parameters for the pseudo-first- and second-order equations and correlation coefficients are tabulated in Table 3 (for Al–DWTS) and Table 4 (for soil). By inspecting R^2 in Tables 3 and 4, it is clear that the pseudo-second-order model is better than the pseudo-first-order model to describe the P adsorption for both Al–DWTS and soil. Several authors have also reported the validity of the pseudo-second-order model in description of P adsorption onto $ZnCl_2$ activated coir pith carbon [3] and recycled Fe(III)/Cr(III) hydroxide [9] as well as alunite [21].

Plots of q_e and r against C_0 were regressed to obtain the values in terms of C_0 with a high regression coefficient for Al–DWTS (R^2 = 0.999, 0.996, respectively). Regressions were gained to the best fitting of q_e and r against C_0 for soil with a slightly lower regression coefficient (R^2 = 0.960, 0.976, respectively). Nevertheless, q_e and r can be expressed as a function of C_0, as shown in Eq. (7) and Eq. (8) for Al–DWTS, and Eq. (9) and Eq. (10) for soil, respectively.

$$q_e = 0.0092 \times C_0 + 0.3784 \qquad (7)$$

$$r = -2 \times 10^{-5} \times C_0{}^{2} + 0.1112 \times C_0 - 2.4243 \qquad (8)$$

$$q_e = 0.0273 \times C_0{}^{0.7264} \qquad (9)$$

$$r = -1 \times 10^{-6} \times C_0{}^{2} + 0.0188 \times C_0 + 1.9256 \qquad (10)$$

Substituting the values of q_e and r into Eq. (6), the relationship of q_t, C_0 and t can be represented for Al–DWTS (Eq. (11)) and soil (Eq. (12)) as follows:

$$q_t = \frac{t}{1/(-2 \times 10^{-5} \times C_0{}^{2} + 0.1112 \times C_0 - 2.4243) + (1/(0.0092 \times C_0 + 0.3784)) \times t} \qquad (11)$$

$$q_t = \frac{t}{1/(-1\times10^{-6}\times C_0{}^2 + 0.0188\times C_0 + 1.9256) + (1/(0.0273\times C_0{}^{0.7264}))\times t} \quad (12)$$

These equations can then be used to derive the amount of P adsorbed on Al–DWTS and soil at any given C_0 (from 69 to 3,425 mg P L^{-1}) and *t*.

3.4. Adsorption isotherm

To assess the adsorption potential of Al–DWTS and soil for high–P solution, Langmuir and Freundlich isotherms were used for fitting sorption equilibrium data. Equations (13) and (14) respectively give the linear forms of the Langmuir isotherm and the Freundlich isotherm.

$$\frac{C_e}{q_e} = \frac{1}{Q_0 b} + \frac{C_e}{Q_0} \quad (13)$$

$$\log q_e = \log k_d + (1/n)\log C_e \quad (14)$$

where q_e is defined as before (mg P g^{-1}), *b* (L mg^{-1}) a sorption constant related to P binding energy, Q_0 the maximum adsorption capacity (mg P g^{-1} sludge) and C_e is the equilibrium P concentration (mg P L^{-1}). The slope and the intercept of the plot of (C_e/q_e) versus C_e gives the values of Q_0 and *b*. k_d is the distribution coefficient, and *n* is a parameter of the Freundlich model.

By fitting the equilibrium data at 23, 30 and 37 ℃ with Eq. (13) and Eq. (14), respectively, the isotherms for Al–DWTS and soil are generated. Figures 6 and 7 illustrate this. Table 5 lists the theoretical parameters of isotherms along with correlation coefficients. It is seen that the experimental data of P adsorption onto the Al–DWTS and the soil could be well fitted by the two models. The Freundlich isotherm exhibited a better fitting than Langmuir isotherm, and this is in agreement with that reported recently by Mortula and Gagnon [22] in a similar study. In addition,

Table 5 also shows that the adsorption capacity increased from 39.4 to 42.9 mg P g^{-1} for Al–DWTS and from 9.49 to 11.03 mg P g^{-1} for soil when the temperature was increased from 23 to 37 ℃.

4. Discussion

The aim of this study was to provide comparative data on P adsorption by Al–DWTS and a local soil. A series of adsorption experiments were designed and in particular, from the results, the Al–DWTS was found to be capable of removing P even at a very high P level. Table 5 shows that the P adsorption capacity of Al–DWTS (39.4 mg P g^{-1}) is more than four times greater than that of soil (9.5 mg P g^{-1}). Although various factors can contribute to P retention mechanisms in the Al–DWTS and soil, it is believed that aluminium oxide is the major cause because it is particularly strong in binding P through ligand exchange and precipitation reactions, which have been investigated previously [23, 24]. Table 1 shows that Al in Al–DWTS is eight-fold greater than that in soil. Although the properties of Al–DWTS are variable and dependent upon the characteristics of the raw waters and the coagulant used, which is believed to result in different P adsorption capacities, it is reasonable to conclude that the alum based DWTS has a very high P adsorption capacity over soil due to the feature of significantly high Al content. As such, the feasibility of augmenting soil's P sorption capacity by mixing DWTS into soils as a new chemical-based P immobilization method has already been investigated and confirmed by different researchers [10–12, 25]. In addition, the specific surface area (SSA) of the Al–DWTS tested was in the range of 49.0–62.3 m^{2} g^{-1} [26]. Although the SSA of the soil was not monitored, in comparison to the range of SSA of other materials reported in literature such as 2.6–3.9 m^{2} g^{-1} [27] and 6.8–31.4 m^{2} g^{-1} [28], the Al–DWTS used herein can be seen to have a comparatively higher SSA. This is believed to be relevant to the high P adsorption capacity.

With regard to the factors that affect the P adsorption behaviour on Al–DWTS and soil, initial concentrations, contact time, pH and temperature have all shown pronounced effects on the adsorption capacity of both adsorbents (see Figs 1–3, Tables 2, 5). In particular, computed models (Eq. (11) and (12)) derived from the data of this study have provided a quantitative description of the integrated effect of some major factors especially the initial P concentration on adsorption behaviour. Although P adsorption is a complicated process, ligand exchange may be the dominating mechanism [23]; more Al content in Al–DWTS may provide more activated exchange sites than soil. From Figs 1 and 2, it seems that when P adsorptions on Al–DWTS and soil occur at lower concentration, the time required to achieve a definite fraction of equilibrium is independent of initial concentration. It is reasonable to expect that at lower concentration, the ratio of the initial number of P molecules to the available exchange sites is low and subsequently the fractional adsorption becomes independent of initial concentration. But, at a higher concentration, fewer exchange sites are available to occupy, so the amount of P adsorbed is dependent upon the initial concentration. In a previous study [15], P adsorption capacity of 10.2 mg PO_4^{3-} g^{-1} Al–DWTS was obtained at a low P concentration which simulated the typical P level in municipal wastewater. This reflects the effect of initial P concentration on adsorption capacity.

The amount of P absorbed onto Al–DWTS and soil increased with an increase of agitation time before equilibrium was reached (Figs 1 and 2). P was initially adsorbed by the activated exchange sites in the exterior surface. When the adsorption at the exterior surface reached the saturation level, P begins to diffuse into the pores within the particles. The determination of pore size distribution of the Al–DWTS indicated that pores with sizes less than 5.98 nm contributed 50% of the surface area while pores of size less than 9.67 nm contributed 90% of the surface area. The pore size larger than 20 nm only contributed an insignificant amount to the surface area [26]. Through the intra-particle diffusion study [29, 30], an intra-particle diffusion coefficient k_{id} is given by the equation:

$$q_t = k_{id} t^{1/2} \tag{15}$$

Figures 8 and 9 show the plots of q_t versus $t^{1/2}$ for Al–DWTS and soil, respectively. Table 6 lists the calculated intra-particle diffusion coefficient k_{id} values. Figures 8 and 9 reveal two separate regions active in the P adsorption process on Al–DWTS and soil at high initial concentration. The initial portion is attributed to the mass transfer of P molecules from bulk solution to absorbent surface; the second portion is the intra-particle diffusion on the absorbent. It is believed that the intra-particle diffusion might be the rate-controlling step in the P adsorption process. As mentioned previously, the pH of the aqueous solution is an important variable that influences the P adsorption on Al–DWTS and soil. As Fig. 3 shows, the amount of P adsorbed onto Al–DWTS and soil tends to decrease when pH increases from 4.0 to 9.0. In an early study [23], the increase of OH^- in solution could affect the electrostatic properties of the sludge, which makes the surface charge of the Al–DWTS change from positive to negative. This is confirmed by measuring the zeta potential, which ranged from +75.8 to –33.7 mV corresponding to a pH change from 4.3 to 9.0. The more negatively charged surface would repulse the negatively charged species (such as PO_4^{3-}) in solution to break the P-binding process.

Although chemical precipitation of the various forms of calcium phosphates is favoured at a pH above 7.5 [31], this is not the case for the Al–DWTS and soil studied in spite of the reasonably high contents of calcium in Al–DWTS and soil (see Table 1). It is noted in Fig. 3 that when pH < 4.0, such as pH = 3.0, the P adsorption capacity of Al–DWTS and soil decreases. This may be caused by a higher solubility of aluminium oxide as it occurs below a pH value of about 4.0–4.5 [8, 32]. The effect of temperature on the P adsorption capacity of Al–DWTS and Bailieborough soil shows (in Table 5) that the sorption of phosphate is an endothermic process. Yet, although the P adsorption on Al–DWTS tends to increase with increased temperature from 23 ℃ to 37 ℃, there is a relatively slight increase on soil. The sorption constant *b*, which relates to the P binding energy, increased from 0.0156 to 0.0190 L mg^{-1} for Al–DWTS and increased from 0.0022 to 0.0029 L mg^{-1} for soil at adsorption conducted at temperatures from 23 ℃ to 37 ℃. This suggests that increasing temperature favours the P sorption.

5. Conclusions

An aluminium coagulated drinking water treatment sludge (Al–DWTS) and a constructed wetland soil were assessed for their P removing ability. The same trends of P adsorption were obtained in both cases. But, the Al–DWTS exhibited a significant P immobilization ability at high-P concentration in contrast to the soil. P adsorption capacity on Al–DWTS in high-P solution is 39.4 mg P g^{-1}, which is more than four times greater than the value (9.14 mg P g^{-1}) on soil. Analysis of kinetic data showed that uptake of P onto Al–DWTS and soil followed pseudo-second-order kinetics. Equilibrium adsorption data of Al–DWTS and soil obey both Langmuir and Freundlich isotherms with the Freundlich isotherm being better than the Langmuir. Maximum P removal occurred at pH = 4.0 for both adsorbents tested. The sorption capacity of both Al–DWTS and soil increases at a temperature range from 23 to 37 ℃. Overall, this result provides the technical support for using

Al–DWTS to benefit soil as an absorbent for removal of P in a wider range of concentration from P-rich wastewaters.

Acknowledgements

The authors would like to thank the Irish Environmental Protection Agency for financial support of this study (Grant no: 2005-ET-MS-38-M3); and also Dr J.F. Fu and Dr A.O. Babatunde for their assistance during the manuscript preparation. Many thanks also go to Mr. P. Kearney, section head technician of the Water and Effluents Laboratory, UCD, for his invaluable technical assistance during the study.

References

[1] Eilbeck, W.J. and Mattock, G., 1981, *Chemical Process in Wastewater Treatment*; Wiley: New York, 271–276.

[2] Yeoman, S., Stephenson, T., Lester, J.N. and Perry, R., 1988, The removal of phosphorus during wastewater treatment: review. *Environmental Pollution*, **49**, 183–233.

[3] Namasivayam, C. and Sangeetha, D., 2004, Equilibrium and kinetic studies of adsorption of phosphate onto $ZnCl_2$ activated coir pith carbon. *Journal of Colloid Interface Science*, **280**, 359–365.

[4] Bhargava, D.S. and Sheldarkar, S.B., 1993, Use of TNSAC in phosphate adsorption studies and relationships: literature, experimental methodology, justification and effects of process variables. *Water Research*, **27**, 303–312.

[5] Ugurlu, A. and Salman, B., 1998, Phosphorus removal by fly ash. *Environment International*, **24**,

911–918.

[6] Oguz, E., 2005, Sorption of phosphate from solid/liquid interface by fly ash. *Colloids and Surfaces A: Physicochemical and Engineering Aspects*, **262**, 113–117.

[7] Zeng, L., Li, X. and Liu, J., 2004, Adsorptive removal of phosphate from aqueous solutions using iron oxide tailings. *Water Research*, **38**, 1318–1326.

[8] Özacar, M., 2003, Adsorption of phosphate from aqueous solution onto alunite. *Chemosphere*, **51**, 321–327.

[9] Namasivayam, C. and Prathap, K., 2005, Recycling Fe(III)/Cr(III) hydroxide, an industrial solid waste for the removal of phosphate from water. *Journal of Hazardous Materials*, **B123**, 127–134.

[10] Novak, J.M. and Watts, D.W., 2004, Increasing the phosphorus sorption capacity of Southeastern coastal plain soils using water treatment residuals. *Soil Science*, **169**, 206–214.

[11] Novak, J.M and Watts, D.W., 2005, An alum-based water treatment residual can reduce extractable phosphorus concentration in three phosphorus-enriched coastal plain soils. *Journal of Environmental Quality*, **34**, 1820–1827.

[12] Makris, K.C., Harris, W.G., O’Connor, G.A. and Obreza, T.A., 2004, Phosphorus immobilization in micropores of drinking-water treatment residuals: Implications for long-term stability. *Environmental Science and Technology*, **38**, 6590–6596.

[13] Ippolito, J.A., Barbarick, F.A., Heil, D.N., Chandler, J.P. and Redente, E.F., 2003, Phosphorus retention mechanisms of a water treatment residual. *Journal of Environmental Quality*, **32**, 1857–1864.

[14] Dayton, E.A. and Basta, N.T., 2005, A method for determining the phosphorus sorption capacity and amorphous aluminium of aluminium-based drinking water treatment residuals. *Journal of*

Environmental Quality, **34**, 1112–1118.

[15] Yang, Y., Tomlinson, D., Kennedy, S. and Zhao, Y.Q., 2006, Dewatered alum sludge: a potential adsorbent for phosphorus removal. *Water Science and Technology*, **54**(5), 207–213.

[16] Razali, M., Zhao, Y.Q. and Bruen, M., 2007, Effectiveness of drinking-water treatment sludge in removing different phosphorus species from aqueous solution. *Separation and Purification Technology*, **55**, 300–306.

[17] Zhao, Y.Q., Babatunde, A.O., Razali, M. and Harty, F., 2008, Use of dewatered alum sludge as a substrate in reed bed treatment systems for wastewater treatment. *Journal of Environmental Science and Health, Part A: Toxic/Hazardous Substances and Environmental Engineering*, **43**, 105–110.

[18] Zhao, Y.Q., Zhao, X.H. and Babatunde, A.O., 2009, Use of dewatered alum sludge as main substrate in treatment reed bed receiving agricultural wastewater: Long-term trial. *Bioresource Technology*, **100**, 644–648.

[19] IWA. *Constructed wetlands for pollution control: Processes, Performance, Design and Operation.* IWA Specialist Group on Use of Macrophytes in Water Pollution Control. London: IWA Publishing, 2000.

[20] Özacar，M., 2003, Equilibrium and kinetic modelling of adsorption of phosphorus on calcined alunite. *Adsorption*, **9**, 125–132.

[21] Özacar, M., 2006, Contact time optimization of two-stage batch adsorber design using second-order kinetic model for the adsorption of phosphate onto alunite. *Journal of Hazardous Materials*, **137**, 218–225.

[22] Mortula, M.M. and Gagnon, G.A., 2007, Alum residuals as a low technology for phosphorus removal from aquaculture processing water. *Aquacultural Engineering*, **36**, 233–238.

[23] Yang, Y., Zhao, Y.Q., Babatunde, A.O., Wang, L., Ren, Y.X. and Han, Y., 2006, Characteristics and mechanisms of phosphate adsorption on dewatered alum sludge. *Separation and Purification Technology*, **51**, 193–200.

[24] Dustin, L.H. and Jim, J.W., 2006, Fractionation and sorption of inorganic phosphorus in Louisiana calcareous soils. *Soil Science*, **171**, 39–51.

[25] DeWolfe, J., 2006, *Water Residuals to Reduce Soil Phosphorus*, AWWA Research Foundation, IWA Publishing.

[26] Yang, Y., Zhao, Y.Q. and Kearney, P., 2008, Influence of ageing on the structure and phosphate adsorption capacity of dewatered alum sludge. *Chemical Engineering Journal*, **145**, 276–284.

[27] Roger, R., 2000, Shell sand: A new filter medium for constructed wetlands and wastewater treatment. *Journal of Environmental Science and Health, Part A: Toxic/Hazardous Substances and Environmental Engineering*, **35**, 1335–1355.

[28] Drizo, A., Frost, C.A., Grace, J. and Smith, K.A., 1999, Physico-chemical screening of phosphate-removing substrates for use in constructed wetland systems. *Water Research* **33**, 3595–3602.

[29] Weber, W.J. and Morris, J.C., 1963, Preliminary appraisal of advanced waste treatment processes. *Water Pollution Research*, **2**, 231–241.

[30] Makris, K.C., El-Shall, H., Harris, W.G. and Obreza, T.A., 2004, Intraparticle phosphorus diffusion in a drinking water treatment residual at room temperature. *Journal of Colloid and Interface Science*, **277**, 417–423.

[31] Stumm, W. and Morgan, J.J., 1981, *Aquatic Chemistry. An introduction emphasizing chemical equilibria in natural waters*, 2nd ed. Wiley; New York.

[32] Cheung, K.C. and Venkitachalam, T.H., 2000, Improving phosphate removal of sand in filtration system using alkaline fly ash. *Chemosphere*, **41**, 243–249.

Tables:

Table 1 Principal chemical compositions of Al–DWTS and soil (*DM denotes dry mass)

Chemical composition	Unit	Amount	
		Al–DWTS	Soil
Aluminium (Al)	mg kg-DM^{-1}*	42,880.0	5,409.0
Iron (Fe)	mg kg-DM^{-1}	2,465.0	2,231.0
Calcium (Ca)	mg kg-DM^{-1}	1,964.0	3,400.0
Magnesium (Mg)	mg kg-DM^{-1}	227.4	3,696.0
Lead (Pb)	mg kg-DM^{-1}	4.8	5.3
Arsenic (As)	mg kg-DM^{-1}	23.6	1.4
Mercury (Hg)	mg kg-DM^{-1}	N/A	< 0.4
Sulphur (S)	mg kg-DM^{-1}	18.9	4,759.0
Chlorine (Cl)	mg kg-DM^{-1}	16.0	11.7
Phosphorus (P)	mg kg-DM^{-1}	154	2,400.0
Moisture content	%	25.5	15.5
Loss in dry mass on ignition	%	49–57	N/A

Table 2 P adsorption capacity of Al–DWTS and soil at different initial concentrations (T = 23 ℃, pH = 4.0)

Initial concentration (mg P L^{-1})	P adsorption capacity, q_e (mg P g^{-1})	
	Al–DWTS	Soil
69	0.67	0.52
343	3.32	2.28
856	8.37	3.67
1,142	11.08	4.56
1,712	16.60	8.35
3,425	31.64	8.15

Table 3 Kinetic parameters for the removal of P by Al–DWTS (T = 23 ℃, pH = 4.0)

C_0 (mg P L^{-1})	First-order model		Second-order model		
	k_1 (h^{-1})	R^2	r (mg g^{-1} h^{-1})	k_s (g mg^{-1} h^{-1})	R^2
69	1.58	0.970	6	13.37	0.995
343	1.38	0.967	30	2.72	0.999
856	1.14	0.985	75	1.07	0.998
1,142	0.90	0.946	96	0.78	0.998
1,712	0.87	0.967	112	0.41	0.999
3,425	0.72	0.943	86.9	0.09	0.999

Table 4 Kinetic parameters for the removal of P by soil (T = 23 ℃, pH = 4.0)

C_0 (mg P L^{-1})	First-order model		Second-order model		
	k_1 (h^{-1})	R^2	r (mg g^{-1} h^{-1})	k_s (g mg^{-1} h^{-1})	R^2
69	2.23	0.990	3.86	14.3	0.995
343	1.59	0.990	7.85	1.51	0.998
856	3.15	0.997	17.8	1.32	0.998
1,142	1.95	0.973	21.7	1.04	0.999
1,712	1.17	0.977	35.6	0.51	0.999
3,425	0.70	0.874	54.4	0.82	0.999

Table 5 Langmuir and Freundlich isotherms constants obtained at obtained pH = 4.0

Adsorbent	T	Langmuir			Freundlich		
	(℃)	Q_0 (mg P g^{-1})	b	R^2	k_d	1/n	R^2
Al–DWTS	23	39.4	0.0156	0.973	0.994	0.668	0.986
	30	40.7	0.0167	0.962	1.137	0.661	0.989
	37	42.9	0.0190	0.969	1.316	0.655	0.985
Soil	23	9.5	0.00220	0.931	0.125	0.563	0.938
	30	10.1	0.00256	0.942	0.163	0.541	0.945
	37	11.0	0.00293	0.962	0.210	0.514	0.945

Table 6 Intraparticle diffusion rate coefficient of P adsorption on Al–DWTS and soil (T = 23 ℃, pH = 4.0)

C_0(mg P L^{-1})	Al–DWTS		Soil	
	k_{id}	R^2	k_{id}	R^2
69	0.12	0.94	0.10	0.85
343	0.45	0.97	0.56	0.94
856	1.37	0.86	0.65	0.92
1,142	1.71	0.88	0.77	0.92
1,712	1.99	0.91	1.52	0.99
3,425	6.22	0.95	0.98	0.95

Figure Captions:

Fig. 1. Time variation of P-adsorption at various initial P concentrations for Al–DWTS (T = 23 ℃, pH = 4.0)

Fig. 2. Time variation of P adsorption at various initial P concentrations for soil (T = 23 ℃, pH = 4.0)

Fig. 3. Effect of pH on P-adsorption onto Al–DWTS and soil (C_0 = 3,425 mg L^{-1}, T = 23 ℃)

Fig. 4. Plot of the pseudo-second-order adsorption kinetics of P on Al–DWTS at different initial concentrations (T = 23 ℃, pH = 4.0)

Fig. 5. Plot of the pseudo-second-order adsorption kinetics of P on soil at different initial concentrations (T = 23 ℃, pH = 4.0)

Fig. 6. Langmuir (upper) and Freundlich (lower) adsorption isotherms of P adsorption onto Al–DWTS at different temperatures (pH = 4.0)

Fig. 7. Langmuir (upper) and Freundlich (lower) adsorption isotherms of P adsorption onto soil at different temperatures (pH = 4.0)

Fig. 8. Intraparticle diffusion plot for the P adsorption on Al–DWTS (T = 23 ℃, pH = 4.0)

Fig. 9. Intraparticle diffusion plot for the P adsorption on soil (T = 23 ℃, pH = 4.0)

Figures:

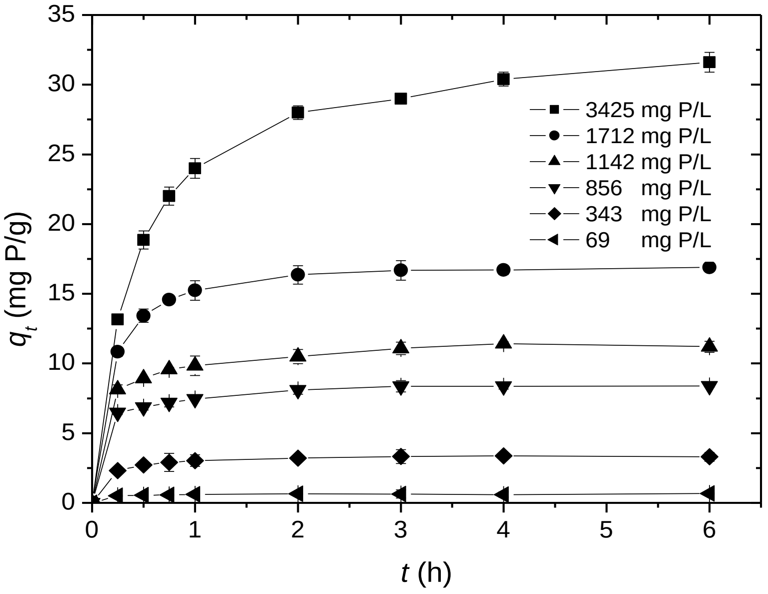

Fig. 1.

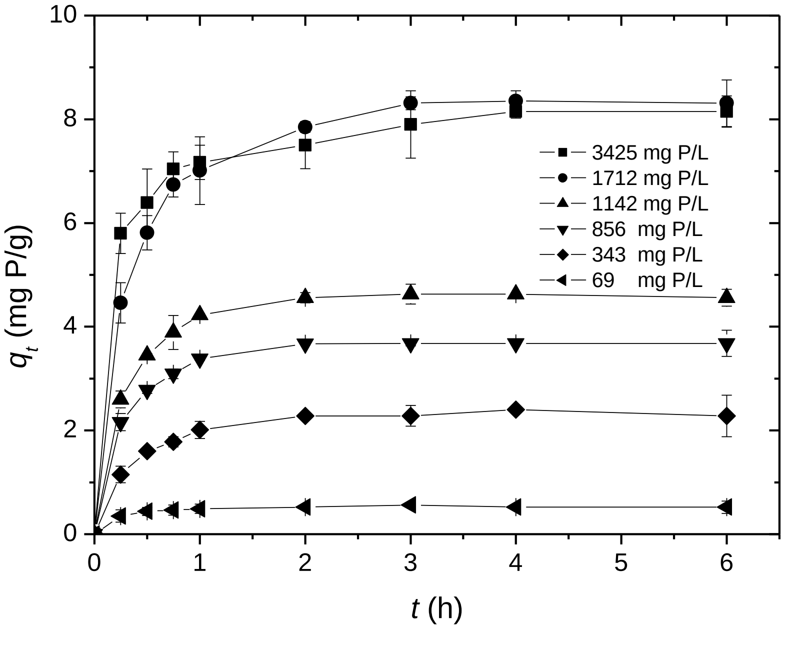

Fig. 2.

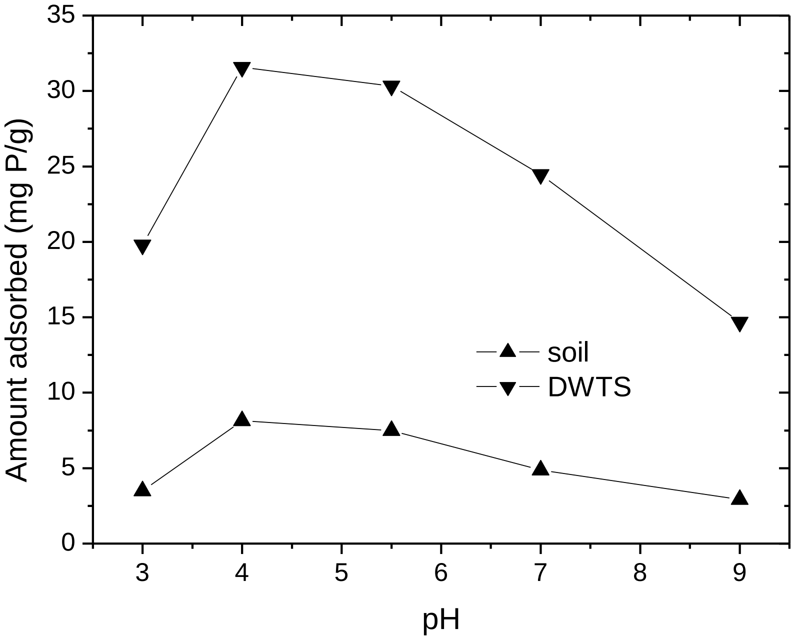
Amount adsorbed (mg P/g)
pH
soil
DWTS
0
5
10
15
20
25
30
35
3
4
5
6
7
8
9

Fig. 3.

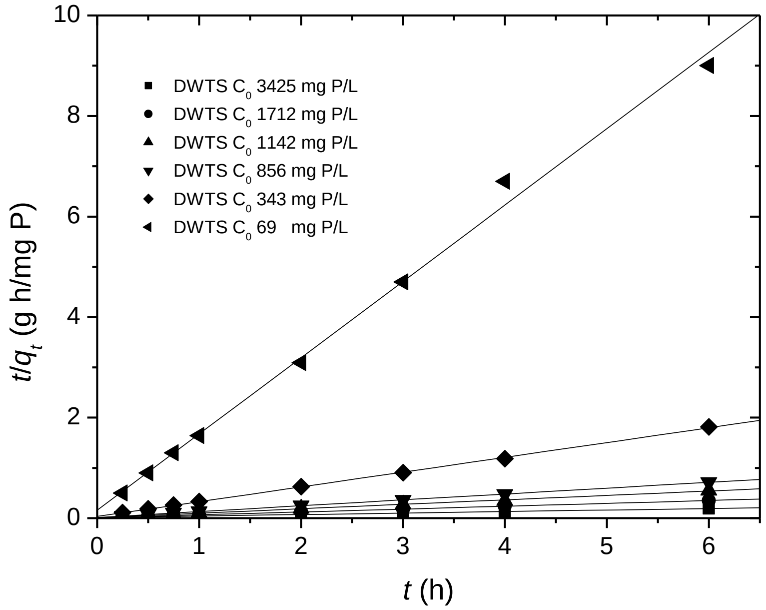
t/q_t (g h/mg P)
t (h)
DWTS C_0 3425 mg P/L
DWTS C_0 1712 mg P/L
DWTS C_0 1142 mg P/L
DWTS C_0 856 mg P/L
DWTS C_0 343 mg P/L
DWTS C_0 69 mg P/L
0
2
4
6
8
10
0
1
2
3
4
5
6

Fig. 4.

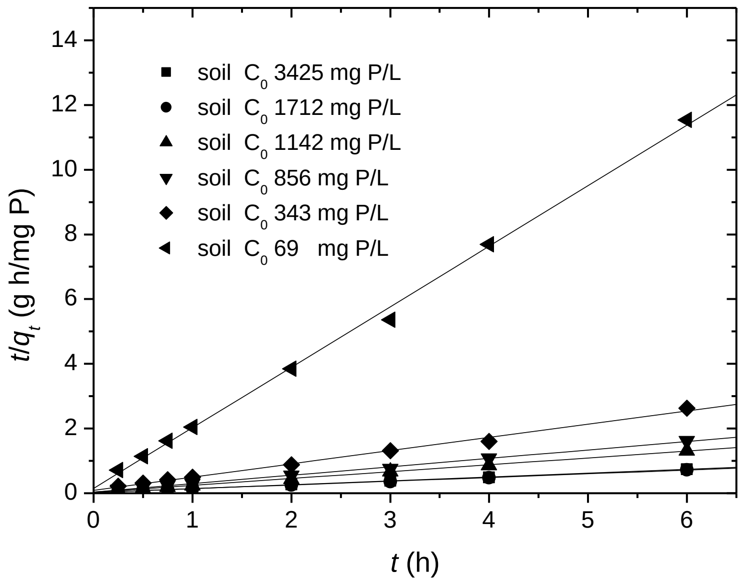
14
12
10
8
6
4
2
0
0
1
2
3
4
5
6
t/q_t (g h/mg P)
t (h)
■ soil C_0 3425 mg P/L
● soil C_0 1712 mg P/L
▲ soil C_0 1142 mg P/L
▼ soil C_0 856 mg P/L
◆ soil C_0 343 mg P/L
◀ soil C_0 69 mg P/L

Fig. 5.

446

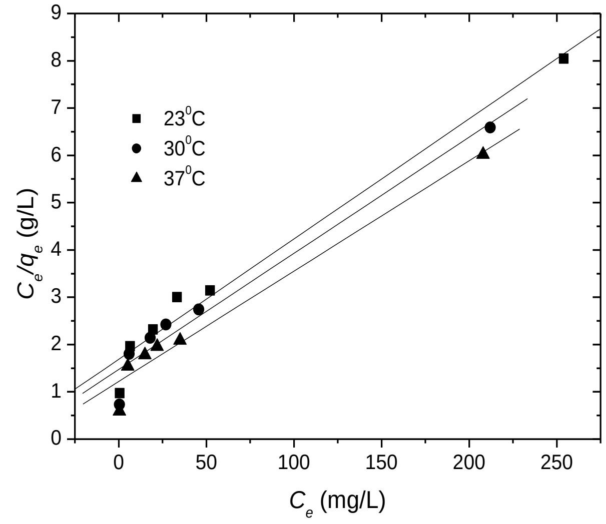

447

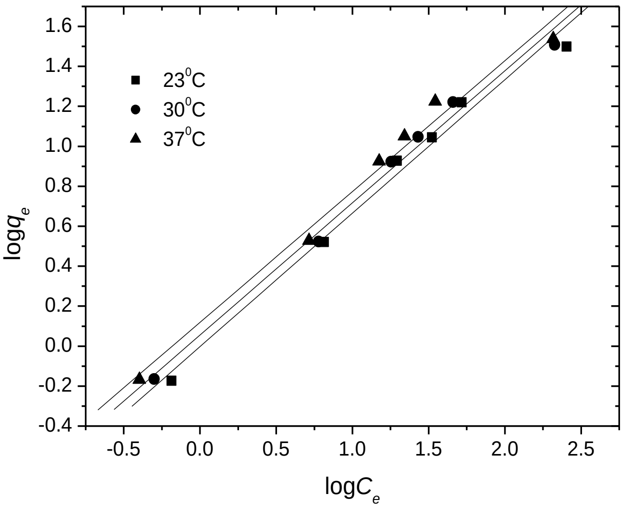

448

449 **Fig. 6.**

450

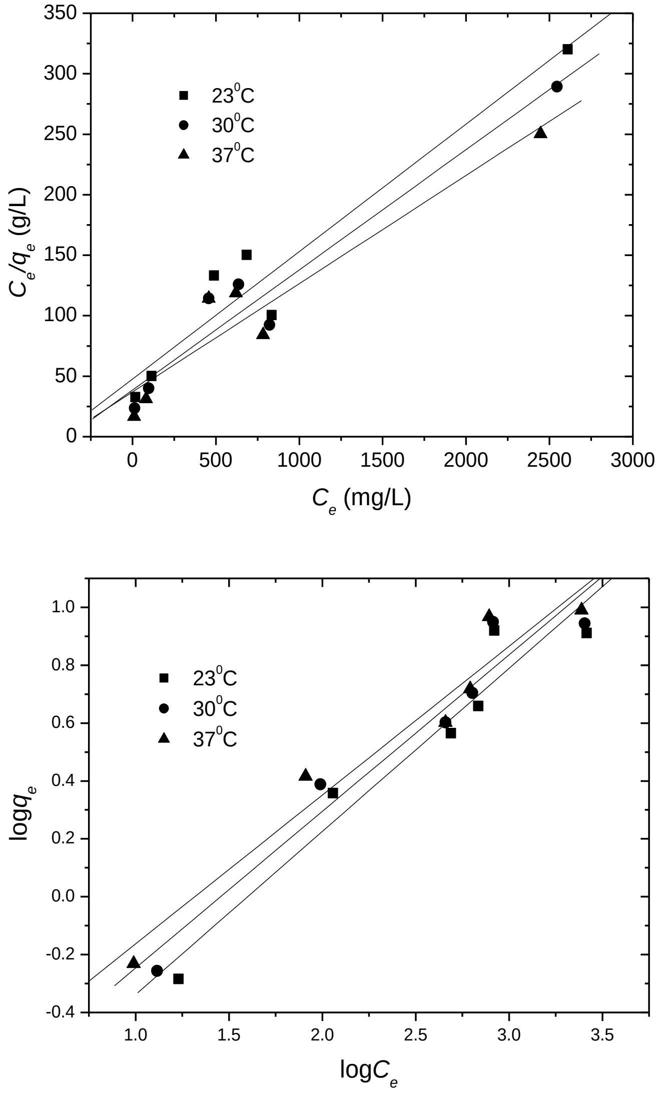
350
300
250
200
150
100
50
0
C_e/q_e (g/L)
0
500
1000
1500
2000
2500
3000
C_e (mg/L)
■ 23^0C
● 30^0C
▲ 37^0C
1.0
0.8
0.6
0.4
0.2
0.0
-0.2
-0.4
$\log q_e$
1.0
1.5
2.0
2.5
3.0
3.5
$\log C_e$
■ 23^0C
● 30^0C
▲ 37^0C

Fig. 7.

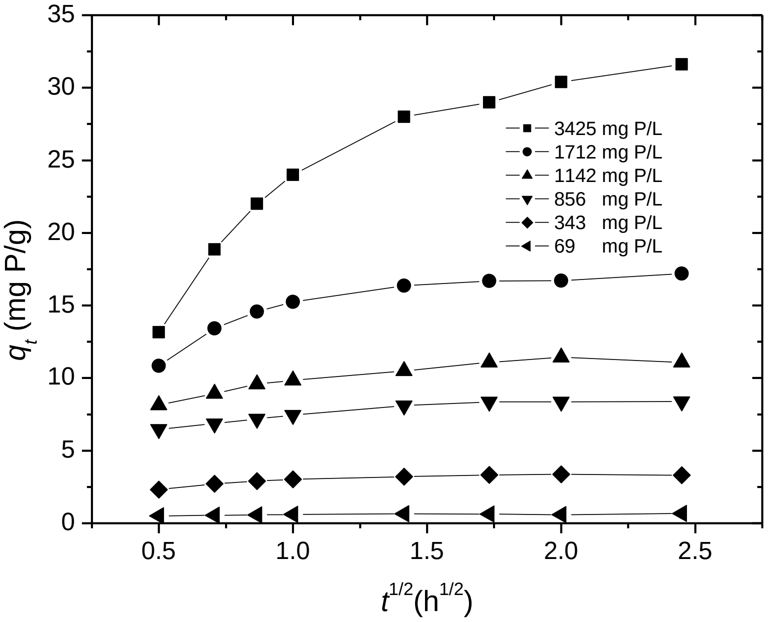

35
30
25
20
15
10
5
0
q_t (mg P/g)
0.5
1.0
1.5
2.0
2.5
$t^{1/2}$(h$^{1/2}$)
3425 mg P/L
1712 mg P/L
1142 mg P/L
856 mg P/L
343 mg P/L
69 mg P/L

Fig. 8.

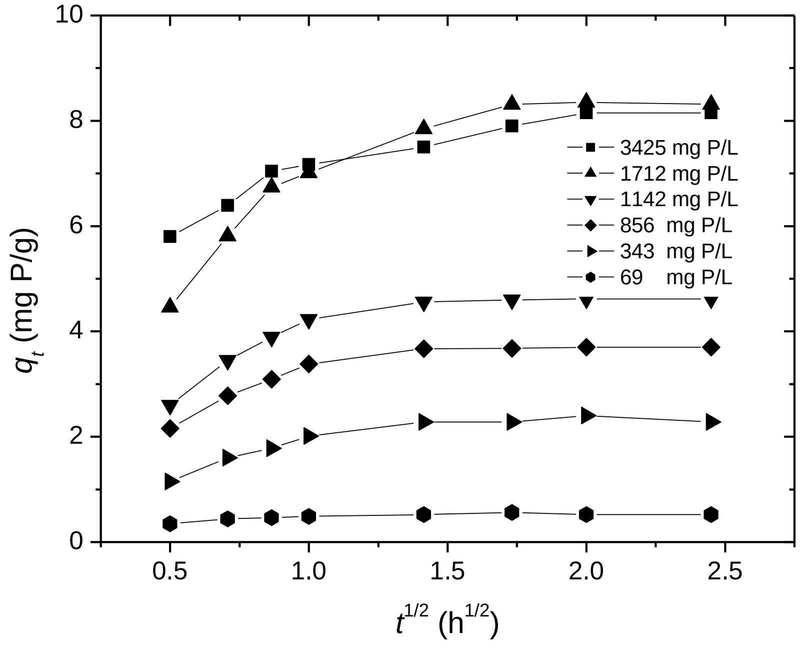

10
8
6
4
2
0
q_t (mg P/g)
0.5
1.0
1.5
2.0
2.5
$t^{1/2}$ (h$^{1/2}$)
3425 mg P/L
1712 mg P/L
1142 mg P/L
856 mg P/L
343 mg P/L
69 mg P/L

Fig. 9.